
Proceedings Paper:
Rai, K, Fairweather, M and Mortimer, LF (2019) Effect of Reynolds Number on Critical Stokes Number Particle Collision Statistics in Multiphase Turbulent Channel Flows. In: Proceedings of ICMF 2019, the 10th International Conference on Multiphase Flow. ICMF 2019, 19-24 May 2019, Rio de Janeiro, Brazil.

Effect of Reynolds Number on Critical Stokes Number Particle Collision Statistics in Multiphase Turbulent Channel Flows

K. Rai, M. Fairweather, L.F. Mortimer

School of Chemical and Process Engineering

University of Leeds, Leeds, LS2 9JT, UK

pmkr@leeds.ac.uk, m.fairweather@leeds.ac.uk, l.f.mortimer@leeds.ac.uk

Keywords: Direct numerical simulation, Lagrangian particle tracking, turbulence, multiphase flow, four-way coupling, interparticle collisions

Abstract

Spherical particle collision statistics in multiphase turbulent channel flows are obtained using a Lagrangian particle tracking algorithm four-way coupled to direct numerical simulations. Two channel flows are simulated at Re_τ=180 and Re_τ=590 with particles of the Kolmogorov Stokes number St_K=1. Particle collision velocities and angles within four regions of the channel flows (viscous sublayer, buffer layer, log-law region and bulk flow) are analysed to elucidate the dynamics of particle interactions in the various regions of the turbulent flows. The results indicate that the most significant contribution to collision velocities arises in the streamwise direction, with particles in the viscous sublayer region colliding with lower streamwise velocities compared to those in other regions of the flow. Furthermore, the spread in the distribution of collision angles is found to be highest in the viscous sublayer, and lowest in the bulk flow region.

Introduction

Multiphase flow simulations allow us to quantitatively and qualitatively study particle-fluid and particle-particle interactions in turbulent flows. In both research and industrial applications, often the primary motivation for conducting such simulations (where possible) is driven by cost savings on expensive experiments, or the difficulty in performing realistic experiments. One such application of relevance to the present work is in the nuclear industry. For example, in the UK most spent fuel and nuclear waste is stored in ponds or silos as a solid-liquid slurry. Over many years the structural integrity of the ponds has been deteriorating and there is an increased need to transport the waste to other safe storage facilities. The problem remains in knowing how best to transport the solid-liquid slurry in the most efficient, effective and safe way. Multi-phase flow simulations can help answer these questions by providing understanding into the behaviour of such systems.

In particle-laden flows one question of interest is at what Stokes number (for a given concentration) do particles start to affect the flow and turbulence dynamics? Over many years simulation-based research has attempted to answer this question. Elghobashi (1994, 2004) has shown that at solid volume fractions between 10^{-6} and 10^{-3} there exists a critical Stokes number, or Kolmogorov Stokes, St_K=1. Below this value, particles are considered small; their response time is much smaller than the Kolmogorov time scale. These particles (due to their low inertia) are prone to becoming trapped in vortical structures of the surrounding fluid. The net effect is that these small particles increase the fluid turbulence kinetic energy and its dissipation rate. Above the critical Stokes number, particles are considered large and they are less likely to respond to local fluctuations in the fluid velocity field and, unlike small particles, they are ejected from vortical structures. The net result is that these large particles attenuate the turbulence kinetic energy and its dissipation rate within the fluid flow.

Other investigations have studied the effect of Stokes number in turbulent flows to determine the extent of modification to the turbulent flow field. For example, Lee & Lee (2015) studied particles with $St^+ = 0.5, 5, 35$ and 125 in a Re_τ=180 channel flow to investigate the physical mechanisms responsible for turbulence enhancement by the particles. They observed that the smallest particles enhance the turbulence by acting as an energy source for high-speed regions in the flow. On the other hand, larger particles attenuate the turbulence field, acting as an energy sink. Zhao et al. (2015) also studied turbulence modification in four-way coupled simulations at various Stokes numbers by varying the particle diameter in homogeneous decaying isotropic turbulence. They observed attenuation at high Stokes numbers even for dilute regimes. Ferrante & Elghobashi (2003) also studied in detail the physical mechanisms responsible for modification of isotropic turbulence at $0.1 \leq St_K \leq 5$.

The literature surrounding particle-fluid and particle-particle interaction mechanisms would be expanded by investigations into the effects of turbulence on four-way coupled particle dynamics around St_K=1. For instance, the effect of Reynolds number on the resulting particle dynamics is not fully understood. Here we attempt to answer the question: how do particles interact differently in low (Re_τ=180) and high (Re_τ=590) Reynolds number flows at St_K=1?

The present work focuses on elucidating particle dynamics by analysing particle-particle collision

statistics of spherical particle-laden flows using various probability distribution functions (PDFs) at St_K=1 at two levels of turbulence in a channel flow.

Methodology

The spectral-element method code Nek5000 (Fischer et al., 2008) was used to perform direct numerical simulations of single-phase channel flows at Re_τ=180 and Re_τ=590. It solves the Navier-Stokes and continuity equation using a 7th order spectral element method. The flow equations are:

$$\frac{\partial u}{\partial t} + u \cdot \nabla u = -\nabla p + \frac{1}{Re} \nabla \cdot \tau + f \qquad (1)$$

$$\nabla \cdot u = 0 \qquad (2)$$

where u is the fluid velocity field, p is pressure, Re is Reynolds number, τ is the viscous deviatoric stress tensor and f is a source term.

The domain properties of both channels are presented in Table 1, where D(x, y, z) is the domain size, N_E is the number of elements and N_N is the equivalent number of nodes, with h being the channel half height.

Table 1: Channel domain simulation parameters.

Re_τ	Re_B	D(x, y, z)	N_E	N_N
180	2800	$14h \times 2h \times 6h$	27×18×23	3.8×10^6
590	11000	$14h \times 2h \times 6h$	61×52×41	45×10^6

Elements close to the wall were distributed more densely to resolve the small scales and more sparsely populated away from the wall (Marchioli et al. 2007). The single-phase flow results were validated against those of Kim et al. (1987), Moser et al. (1999) and Vreman et al. (2014a, 2014b), with good agreement obtained.

Table 2: Kolmogorov-based Stokes number (St_K), and shear (St_τ) and bulk (St_B) Stokes numbers, employed in the simulations.

Re_τ	St_K	St_τ	St_B
180	1	3.94	0.34
590	1	6.67	0.21

For the solid phase, a Lagrangian particle tracking method was employed. The governing equations are:

$$\frac{\partial x_p}{\partial t} = u_p \qquad (3)$$

$$\frac{\partial u_p}{\partial t} = \frac{3 C_D |u_s|}{4 d_p \rho_p} u_s + \frac{3}{4} \frac{C_L}{\rho_p} (u_s \times \omega_f) + \frac{1}{\rho_p} \frac{Du_f}{Dt} + \frac{1}{2\rho_p} \frac{Du_f}{Dt} \qquad (4)$$

Here, x_p is the particle position, C_L is the lift coefficient, ρ_p is the density of a particle, u_f is the velocity of fluid at the position of the particle, u_S is the slip velocity of the particle, u_P is the velocity of the particle, d_p is the particle diameter and ω_f is vorticity. Note that all these quantities are made non-dimensional by the bulk properties of the flow. In Eq. (4), the terms on the right hand side describe the forces acting on the particles, with the first term describing drag, the second term lift, the third pressure gradient and the final term the virtual mass.

Solutions of these equations were coupled with the single-phase flow using the source term in the Navier-Stokes equation, Eq. (1). At every time step the algorithm solves for the single-phase flow and then solves the differential equations, Eqs. (3) and (4), to determine the particle position and velocity using the fourth order Runge-Kutta technique. The source term in Eq. (1) is $f = 1/V_{cell} \sum f_{fp}$, which is summed over the number of particles in V_{cell}, where V_{cell} is the volume of a fluid computational cell and f_{fp} is the force exerted by the fluid on a particle. Two-way coupling was implemented using the point source in cell method developed by Crowe et al. (1977). Particle-particle collisions were modelled using the hard-sphere approach (Sharma et al. 2004, Sundaram & Collins 1996) which models collisions as elastic. There are retroactive and proactive methods for detecting collisions. The former is computationally less intensive but can miss ~20% of the total number of collisions, whilst the latter approach accurately captures collisions, but the hydrodynamic effects of approaching particles are ignored and the method can be computationally expensive for large numbers of collisions. The method employed to detect collisions in the present simulations is a compromise between these two approaches in terms of collision detection rate and computational work.

The algorithm detects collisions between two particles if the distance between their centres (x_p) is less than the diameter of a particle (d_p), $x_p < d_p$, and the velocity at that time step is used to define the collision velocity with the angle between the two velocity vectors obtained using the dot product. The collision velocity is defined as $(|u_{P_1}| + |u_{P_2}|)/2$ and the collision angle is given by $\theta = \arccos(u_{P_1} \cdot u_{P_2})/(|u_{P_1}||u_{P_2}|)$, where $u_{P_1}$and u_{P_2} are the particle velocities. Multiphase flow results for a Re_τ=180 channel flow were validated against the results of Marchioli et al. (2007) at similar Stokes and Reynolds numbers, with good agreement obtained.

The variables used in the plots below are defined as $y^* = y/h$, $y^+ = y^* Re_\tau$, $u^* = u/u_b$, $u^+ = u/u_\tau$, $v^+ = v/u_\tau$ and $w^+ = w/u_\tau$, where h is the half height of the channel. Additionally, u_b is the bulk velocity and u_τ is the shear velocity, with u_p^*, v_p^* and w_p^* normalized by the bulk velocity.

The total number of particles considered was 300,000, each of diameter 0.005*h* giving a volume fraction of 10^{-4}. Their density ratio was chosen to yield St_K=1. St_K is defined as the ratio of the particle response time to the Kolmogorov time scale. Since the Kolmogorov length scale varies across the channel its average was chosen in order to obtain St_K=1. Further details are given in Table 2.

Results and Discussion

In this section we present the results and observations, and discuss the effects of two different Reynolds number flows on particle collision statistics in a four-way coupled multi-phase turbulent channel flow. The results included are single-phase predictions for the Re_τ=590 channel flow, a comparison of the four-way coupled Re_τ=180 flow at St_τ=3.94 with the results of Marchioli et al. (2007) for a one-way coupled Re_τ=150 flow at St_τ=5, and lastly multi-phase results for Re_τ=180 and Re_τ=590, and collision statistics for both Reynolds numbers at critical Stokes, St_K=1 (Table 2).

A. Single-phase flow results

Figure 1 shows the single-phase flow results for the Re_τ=590 channel flow which includes predictions of the streamwise mean velocity together with the root mean square (rms) of the velocity fluctuations and the Reynolds shear stress.

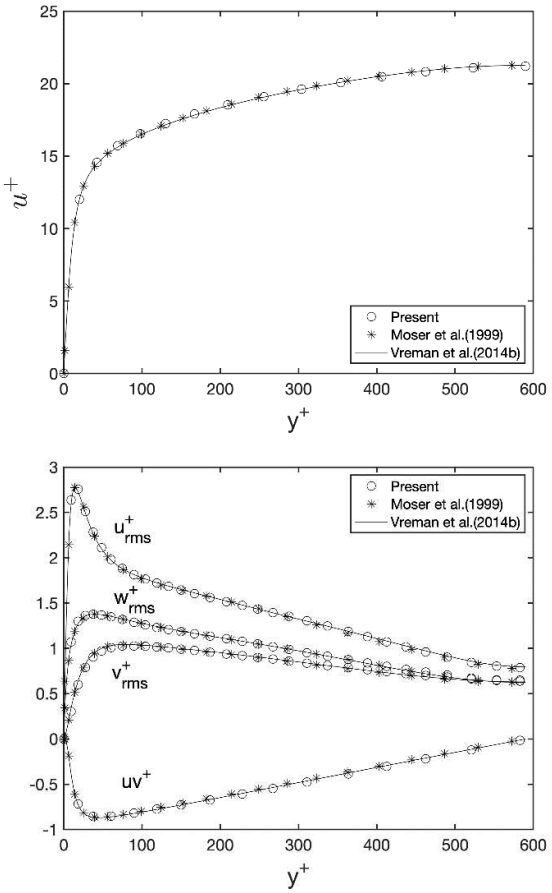

Figure 1: Re_τ=590 single-phase flow statistics and validation. Upper: mean streamwise fluid velocity; lower: rms of velocity fluctuations and shear stress.

Although results for the Re_τ=180 single-phase flow are not presented here, the predictions were qualitatively similar to those of Fig. 1. The results for both the Re_τ=180 and Re_τ=590 flows are in good agreement with DNS predictions from Kim et al. (1987), Vreman et al. (2014a, 2014b) and Moser et al. (1999), as demonstrated in Fig. 1 for the latter case. The notable difference between the Re_τ=180 and Re_τ=590 flows is that in the bulk region at high Reynolds number, the mean streamwise velocity is ~17% greater than in the lower Reynolds number case. Furthermore, although the peak in the streamwise rms velocity fluctuations for both Reynolds number flows occurs at y^+~12 the gradient in these fluctuations after the peak is greater for the high Reynolds number flow, indicating that in near-wall region the Re_τ=590 flow is significantly more turbulent than the Re_τ=180 flow.

B. Multi-phase flow results

Figure 2 compares results for the present four-way coupled Re_τ=180 multi-phase flow with St_τ=3.94 (St_K=1), and the one-way coupled Re_τ=150 multi-phase flow with St_τ=5 of Marchioli et al. (2007).

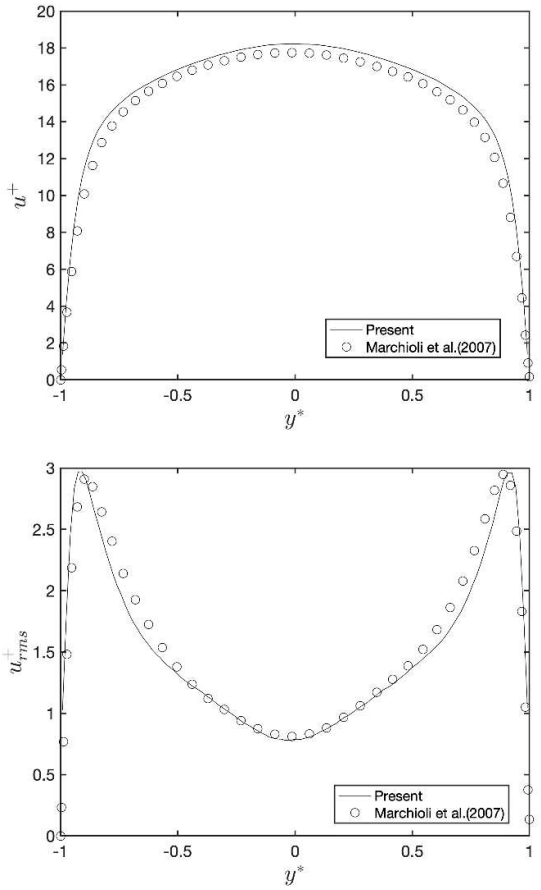

Figure 2: Comparison of four-way coupled Re_τ=180 particle statistics at St_τ=3.94 (St_K=1) with the results of Marchioli et al. (2007) (one-way coupled) at Re_τ=150 and St_τ=5. y^* is coordinate which labels wall normal direction. Upper: particle mean streamwise velocity; lower: rms of particle streamwise velocity fluctuations.

As expected, due to the higher Reynolds number of

the present simulation, the particle mean streamwise velocity is slightly greater than that predicted by Marchioli et al. (2007), although the two profiles are qualitatively similar. However, the streamwise normal stresses are similar in both cases, both qualitatively and quantitatively. The reason for this can be attributed to differences in the level of coupling used in the two cases, and differences in the particle Stokes number between the simulations. In both cases, the peak in the fluctuations is observed to be around y^*~0.9 in the streamwise direction, and at y^*~0.6 in the wall normal and y^*~0.7 in the spanwise directions (not shown). Also, the minimum in the fluctuations is at the centre of the channel, indicating low turbulence level in that region.

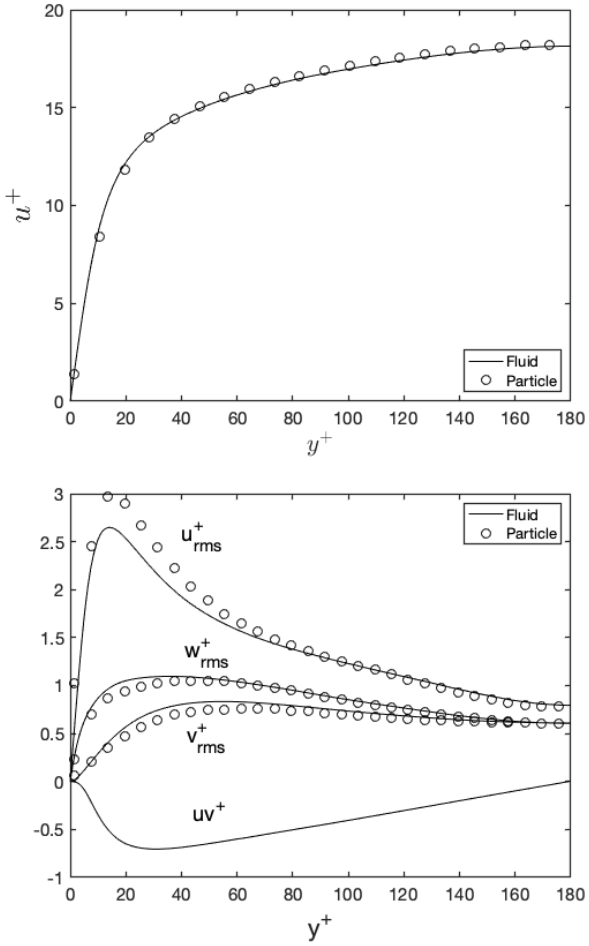

Figure 3: Re_τ=180 multi-phase flow predictions for fluid and particulate phases. Upper: mean streamwise velocity; lower: rms of velocity fluctuations and shear stress.

Error! Reference source not found. and Figure **4** show fluid and particle streamwise mean velocities, as well as the normal and shear stresses, across the channel in the wall normal direction at Re_τ=180 and Re_τ=590, respectively. In both cases, the particles' mean streamwise velocity coincides almost exactly with that of the fluid. In terms of the rms of the velocity fluctuations, although the shape of the profile is unchanged and qualitatively similar to that of the fluid, the particle fluctuations appear to behave differently in the near-wall region in that they exhibit increased streamwise values, whilst the other two normal stress components are slightly reduced relative to the continuous phase. This effect is most noticeable between y^+=0 and y^+=60. This tendency of increased normal stresses in the streamwise direction, and reduced stresses in the other two coordinate directions, has been observed in previous research (e.g. Picciotto et al. 2005). This trend is also observed in both Re_τ flows, although it is less pronounced in the higher Reynolds number case.

Error! Reference source not found.-8 give predicted probability density distribution functions of collision velocities and angles in the two channel flows. Results for the collision statistics are given for four different regions of the channel flows, as defined in Table 3.

Table 3: Channel flow region definitions.

	Re_τ=180		Re_τ=590	
Region	y^+(start)	y^+(end)	y^+(start)	y^+(end)
Viscous	0	5	0	5
Buffer	5	30	5	30
Log-law	30	36	30	200
Bulk	36	180	200	590

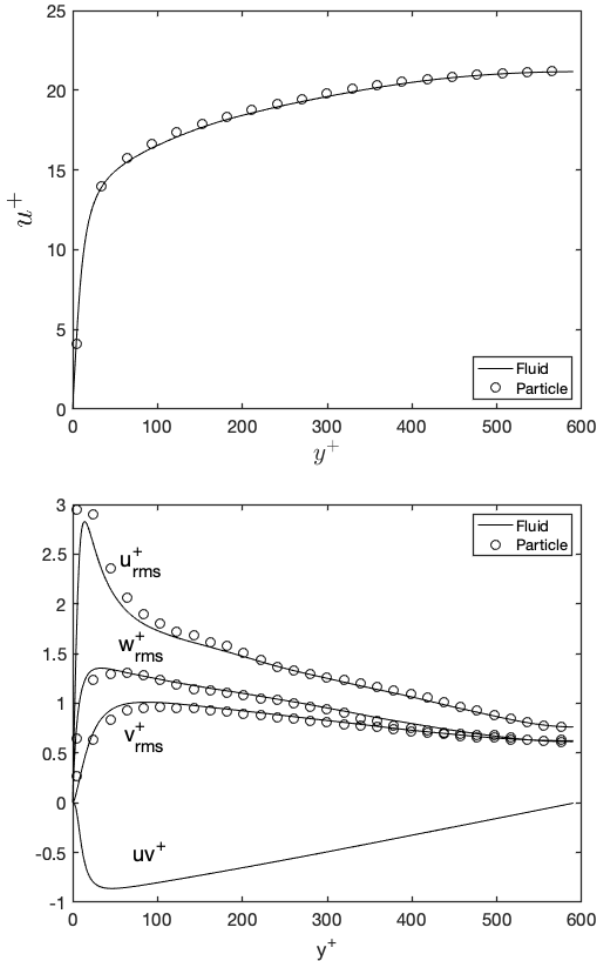

Figure 4: Re_τ=590 multi-phase flow predictions for fluid and particulate phases. Upper: mean streamwise

velocity; lower: rms of velocity fluctuations and shear stress.

Error! Reference source not found. indicates that in the streamwise direction, collision velocities tend to display preferential collision speeds in all regions of the channel. In both Reynolds number flows, as we move from the viscous sublayer to the bulk region, the peak of the distribution increases from $u_p^* \sim 0.1$, 0.4, 0.9 to 1.1. The range of the distribution also changes, with a maximum obtained in the buffer region which narrows in moving to the bulk and viscous sublayer regions. However, in the wall normal (Fig. 6) and spanwise (Fig. 7) directions, the distribution is different to that in the streamwise direction in that the peaks do not shift greatly in moving from the near-wall to the bulk region, tending to be within ~0.0 to 0.02 across the channel.

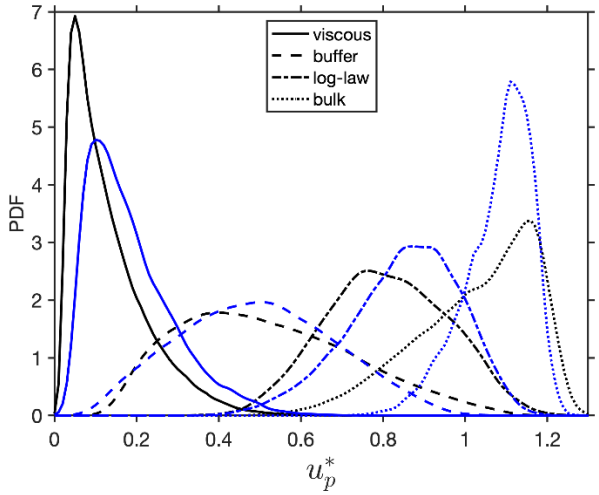

Figure 5: PDFs of streamwise particle collision velocities (u_p^*) in the channel at Re_τ=180 (black) and Re_τ=590 (blue).

In the streamwise direction for the bulk flow region (**Error! Reference source not found.**), the spread in the particle collision velocity distribution for Re_τ=180 is greater than that of the Re_τ=590 simulation, and vice-versa in the viscous sublayer region. This indicates that, on average, the collisions in the Re_τ=590 bulk flow region are much more longitudinal than those in the Re_τ=180 case, and conversely in the viscous sublayer region. This is likely because the high Reynolds number flow has increased bulk flow velocities, and exhibits higher turbulence intensities near the wall, than in the low Reynolds number flow.

Due to relatively high turbulence intensity near the wall in the Re_τ=590 case, the collision velocity distribution (Figure 6 and Figure **7**) is greater than in the Re_τ=180 turbulent flow. However, the results also suggest that in the bulk flow region, the wall normal and spanwise collision velocity distributions are similar, both qualitatively and quantitatively, for the two Reynolds number flows.

Figure 8 demonstrates that as we move from the bulk flow to the viscous sublayer region the spread of the collision angles tends to increase. The viscous and buffer layer regions therefore tend to show a significantly greater spread in this distribution than the log-law and bulk flow regions. The results also suggest that collisions in the buffer layer and the bulk flow regions are the most "head-on", with less spread in the collision angle in predictions for the Re_τ=180 flow. This is to be expected as the higher Reynolds number flow has higher turbulence levels in the near-wall region, as shown in **Error! Reference source not found.** and Figure **4**. The least chaotic collisions, in terms of collision angle, occur in the bulk flow region, where the particles tend to collide longitudinally (i.e. glancing) at ~0.05 degrees in the direction of travel, since the particle momentum in the streamwise direction is sufficiently high, and the fluid fluctuations in other two coordinate directions are relatively low.

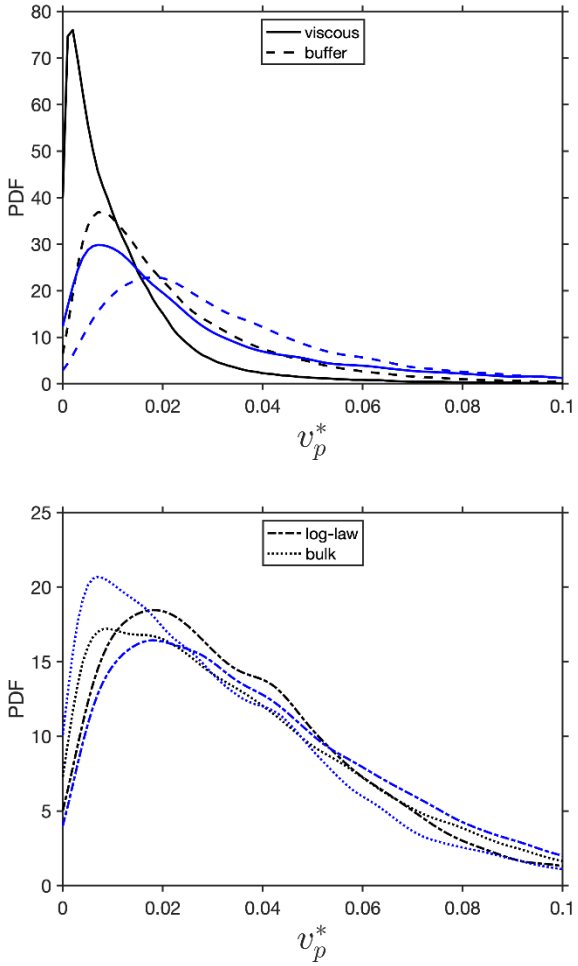

Figure 6: PDFs of wall normal particle collision velocities (v_p^*). Upper: viscous sublayer and buffer layer; lower: log-law and bulk region. Re_τ=180 (black) and Re_τ=590 (blue).

Consideration of all the particle statistics presented allows the following physical insights regarding particle collisions in the presence of low and high Reynolds number turbulent channel flows to be reached:

- The Reynolds number of the flow affects the likelihood of "head-on" collisions, and in moving from the bulk to the near-wall region the spread in collision angles increases significantly.
- The most "head-on" collisions take place in the bulk

flow region at both turbulence levels. The particles collide through glancing interactions in the streamwise direction of travel, with very low fluctuations in the wall normal and spanwise directions.

- Reynolds number does not appear to have much influence on the wall normal and spanwise collision velocities in the bulk region of the flows.

Conclusions

Four-way coupled, particle-laden channel flow simulations at Re_τ=180 and 590 were performed using direct numerical simulation and a Lagrangian particle tracking technique, with particles at St_K=1, to study the effects of Reynolds number on particle collision statistics. The results include PDFs of collision velocities in the streamwise, wall normal and spanwise directions, as well as collision angles, in the viscous sublayer, buffer, log-law and bulk regions of the channel flows.

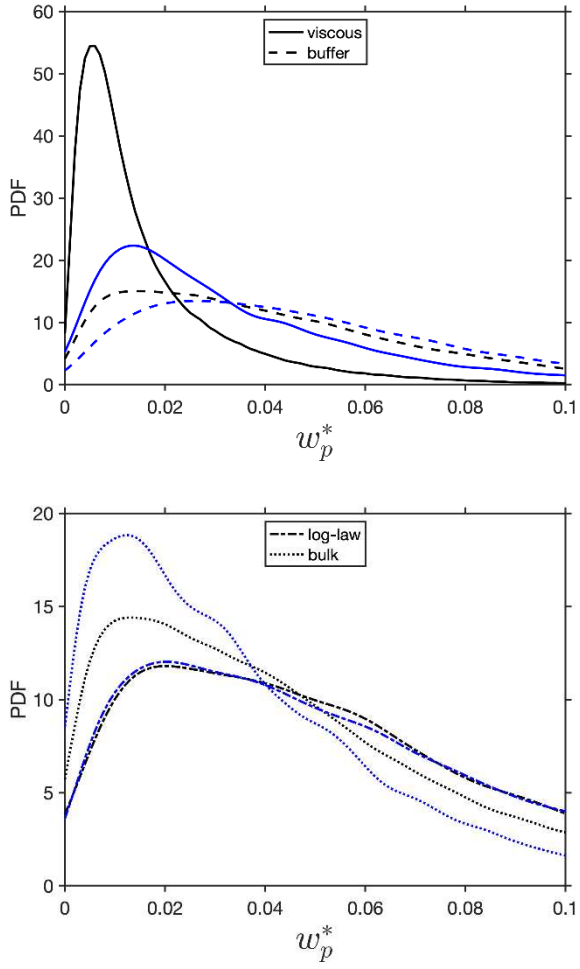

Figure 7: PDFs of spanwise particle collision velocities (w_p^*). Upper: viscous sublayer and buffer layer; lower: log-law and bulk region. Re_τ=180 (black) and Re_τ=590 (blue).

Both low and high Re_τ single-phase flow predictions were in good agreement with the results provided by Kim et al. (1987), Vreman et al. (2014a, 2014b) and Moser et al. (1999). Although both flows were predicted, results were only provided for the high Reynolds number case as the results for both flows were similar in terms of their velocity profiles. Towards the bulk flow region of the channel, the mean streamwise velocity was ~17% greater in the high Reynolds number flow compared to the low Re_τ case. Overall, and relative to the low Reynolds number flow, the peaks in the normal and shear stresses in the high Reynolds number flow were increased and shifted towards the wall. In this case, and beyond y^+~80, the rms of velocity fluctuations and the shear stress tend to decrease linearly, whereas in the low Reynolds number flow only the wall normal and spanwise normal stresses, and the shear stress, display linearity beyond y^+~40.

The multi-phase flow results were compared with the one-way coupled predictions of Marchioli et al. (2007) at St_τ=5 and Re_τ=150 to demonstrate the validity of the particle tracking technique employed. Despite differences in flow parameters and level of coupling between the two simulations, particle results for the mean streamwise velocity and the streamwise normal stress were found to be similar. In comparison with the predictions of Marchioli et al. (2007), therefore, the mean particle streamwise velocity across the channel in the present simulation increased by ~5%, whereas the normal stress was similar in terms of its profile and magnitude.

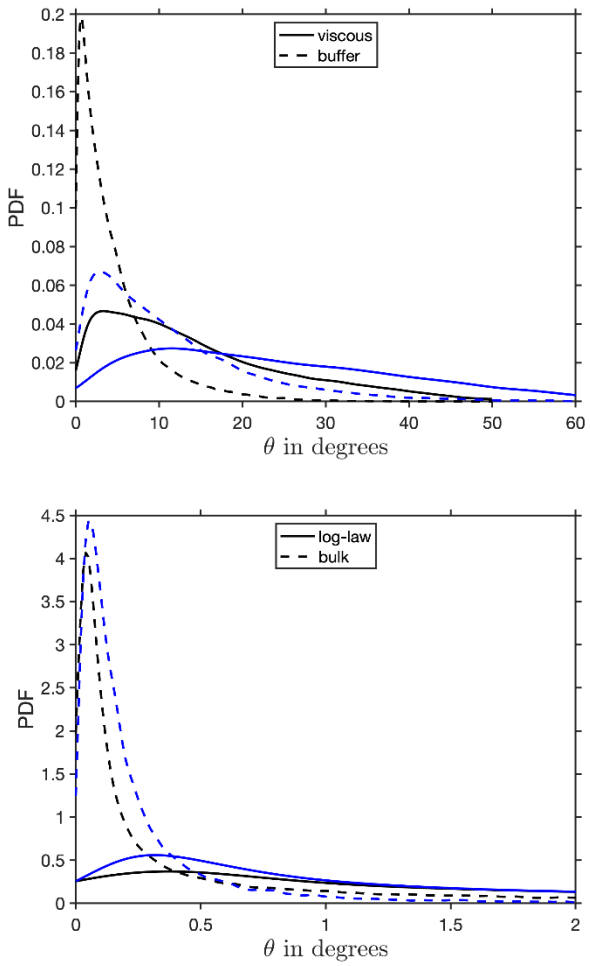

Figure 8: PDFs of collision angles in the channel at

Re_τ=180 (black) and Re_τ=590 (blue).

An increase in the Reynolds number of the flow increases the spread in the distribution of the streamwise collision velocities close to the wall, whilst reducing the spread in the bulk flow region. As we move from the viscous sublayer to the bulk flow region, even though the range of collision velocities is greater in the viscous sublayer for the higher Reynolds number flow, that spread reduces more rapidly than for the low Reynolds number case. The distribution of the spanwise and wall normal collision velocities for both flow Reynolds numbers are similar. In the bulk flow region, particles in the high Reynolds number flow are more likely to collide at higher velocities than particles in Re_τ=180 flow.

The spread in the distribution of the collision angle was found to be lowest in the bulk region and highest in the viscous sublayer region in both low and high Reynolds number flows. In moving from the viscous sublayer to the bulk flow region, this spread tends to reduce, although it is greater for the high Reynolds number case. This indicates that, on average, particle motion is more chaotic in the high Reynolds number flow.

In summary, there is no strong distinction in the distribution of collision statistics between the Re_τ=180 and Re_τ=590 turbulent channel flows. As we move from the bulk flow to the near-wall region, the peak in the streamwise collision velocity distribution shifts from u_p^*~1.1 to 0.1 which, together with velocities in the wall normal and spanwise directions, results in a greater spread in the collision angle distribution in the wall region. Hence, as we move from the bulk flow to the wall region, the particle collisions become more chaotic.

Acknowledgments
The authors are grateful for funding from the UK Engineering and Physical Sciences Research Council through the Centre for Doctoral Training in Nuclear Fission – Next Generation Nuclear (EP/L015390/1).

References

Crowe, C.T., Sharma, M.P. & Stock D.E. The particle-source-in cell (PSI-CELL) model for gas-droplet flows. J. Fluid. Eng., Vol. 99, pp. 325-332 (1977)

Elghobashi, S. On predicting particle-laden turbulent flows. Appl. Sci. Res., Vol. 52, pp. 309-329 (1994)

Elghobashi, S. An updated classification map of particle-laden turbulent flows. Proc. IUTAM Symp. Computational Approaches to Multiphase Flow, Argonne National Laboratory (2004)

Ferrante, A. & Elghobashi, S. On the physical mechanisms of two-way coupling in particle-laden isotropic turbulence. Phys. Fluids, Vol. 15, pp. 315-329 (2003)

Fischer, P.F., Lottes, J.W. & Kerkemeier, S.G. Nek5000 Web page, http://nek5000.mcs.anl.gov (2008)

Kim, J., Moin, P. & Moser, R. Turbulence statistics in fully developed channel flow at low Reynolds number. J. Fluid Mech., Vol. 177, pp. 133-166 (1987)

Lee, J. & Lee, C. Modification of particle-laden near-wall turbulence: Effect of Stokes number. Phys. Fluids, Vol. 27, 23303 (2015)

Marchioli, C., Picciotto, M. & Soldati, A. Influence of gravity and lift on particle velocity statistics and transfer rates in turbulent vertical channel flow. Int. J. Multiphas. Flow, Vol. 33, pp. 227-251 (2007)

Moser, R.D., Kim, J. & Mansour, N.N. Direct numerical simulation of turbulent channel flow up to Re_τ=590. Phys. Fluids, Vol. 11, pp. 943-945 (1999)

Picciotto, M., Marchioli, C., Reeks, M. & Soldati, A. Statistics of velocity and preferential accumulation of micro-particles in boundary layer turbulence. Nucl. Eng. Des., Vol. 235, pp. 1239-1249 (2005)

Sarma, R.L., Winkler, C.M. & Vanka, S.P. A new algorithm for computing binary collisions in dispersed two-phase flows. Numer. Heat Tr. B-Fund., Vol. 45, pp. 99-107 (2004)

Sundaram, S. & Collins, L. R. Numerical considerations in simulating a turbulent suspension of finite-volume particles. J. Comput. Phys., Vol. 124, PP. 337-350 (1996)

Vreman, A.W. & Kuerten, J.G.M. Comparison of direct numerical simulation databases of turbulent channel flow at Re_τ = 180. Phys. Fluids, Vol. 26, 015102 (2014a)

Vreman, A.W. & Kuerten, J.G.M. Statistics of spatial derivatives of velocity and pressure in turbulent channel flow. Phys. Fluids, Vol. 26, 085103 (2014b)

Zhao, F., George, W. K. & Van Wachem, B. G. M. Four-way coupled simulations of small particles in turbulent channel flow: The effects of particle shape and Stokes number. Phys. Fluids, Vol. 27, 83301 (2015)